Honeycomb Sandwich Structure for Future Space Transportation Systems with Integral Cryogenic Tankage

John L. Shideler*
NASA Langley Research Center, Hampton, Virginia
Allan R. Swegle†
Boeing Aerospace Company, Seattle, Washington
and
Roger A. Fields‡
NASA Dryden Flight Research Facility, Edwards Air Force Base, California

This paper presents the status of the structural development of an integral cryogenic-tankage/hot-fuselage concept for future Space Transportation Systems (STS). The concept consists of a honeycomb sandwich structure which serves the combined functions of containment of cryogenic fuel, support of vehicle loads, and thermal protection from an entry heating environment. The inner face sheet is exposed to a cryogenic (LH_2) temperature of $-423°F$ during boost; and the outer face sheet, which is slotted to reduce thermal stress, is exposed to a maximum temperature of 1400°F during a high-altitude, gliding entry. A fabrication process for a René 41 honeycomb sandwich panel with a core solidity less than 1% has been developed, which is consistent with desirable heat treatment processes for high strength. Preliminary structural allowables and thermal properties for use in structural system studies have been determined; two 1×6 ft panels have been tested with combined thermal and mechanical loads; and the effects of slots used to reduce stresses in the outer face sheet on the lower surface of the vehicle have been evaluated in the cryogenic environment associated with containment of LH_2 fuel. Based on the work presented in previous system studies and the hardware development described herein, the René 41 honeycomb sandwich appears to be a viable structural concept for an integral cryogenic-tank/hot-fuselage structure; however, additional in-depth studies, hardware development, and testing are required to verify the concept fully.

Introduction

THE only existing reusable Space Transportation System (STS), the Space Shuttle, employs an aluminum structure insulated from aerodynamic heating generated during ascent and entry by a reusable Thermal Protection System (TPS). The cryogenic fuel used by the Shuttle is carried in the expendable external tank, but future systems designed for full reusability will undoubtedly carry their own cryogenic fuels internally. Consequently, structural design of new fully reusable systems must necessarily address problems associated with containment of cryogenic fuel as well as the conventional considerations of thermal protection and support of vehicle structural loads.

Both insulated and hot-structure design approaches have been studied.[1-6] One such design approach[4] is the hot-structure concept for a single-stage-to-orbit vehicle shown in Fig.1. This concept has followed the design philosophy of using the recently developed Space Shuttle main engines and striving for improvements in structural mass fraction. The concept is an integral tank/fuselage structure which combines the functions of fuel containment, thermal protection, and support of vehicle thrust and aerodynamic loads. The vehicle is designed for a low planform loading, which results in a higher altitude entry trajectory than that flown by the Shuttle Orbiter. This high-altitude, gliding entry results in maximum surface temperatures of only about 1400°F which are within the operating range for the nickel-base superalloy René 41. The structure consists of a vacuum-sealed-cell honeycomb sandwich with the inner skin of the fuselage at a temperature of $-423°F$ due to exposure to the cryogenic fuel and the outer skin at a temperature of 400°F due to exposure to the boost aerothermal environment. These temperature gradients through the thickness of the sandwich during boost conditions produce large thermal stresses which must be accommodated in the design. The thermal stresses have been partially relieved by slotting the outer face sheet on the windward surface of the vehicle fuselage. These slots eliminate biaxial compression stress which would otherwise occur from thermal and pressure loads. (Transverse bending loads are low because LOX is carried in the wings.) The slots are approximately 0.030 in. wide and are sized to be nearly closed when the outer surface of the panel is heated to 1400°F. Pressure loads in the noncircular section are carried by tension struts at each frame location (Fig. 1). Although René 41 is required on the hotter, windward surface, a material with a better strength-to-weight ratio may be preferred on the cooler leeward surface to save weight. (The study of Ref. 4 considers using titanium honeycomb on this surface.)

This paper presents the results of the development of an acceptable fabrication procedure for brazing thin gage René 41 honeycomb sandwich and the results of experimental determination of structural and thermal properties of the sandwich. The ability of the structure to support high combined thermal and mechanical stresses is investigated. Because the outer skin of the sandwich is slotted, the effect of these slots in the cryogenic environment during ground hold and boost is evaluated. The effect of the slots in the hypersonic environment during entry and recommendations for future work are discussed.

Presented as Paper 82-0653 at the AIAA/ASME/AHS 23rd Structures, Structural Dynamics and Materials Conference, New Orleans, La., May 10-12, 1982; submitted May 24, 1982; revision received Sept. 20, 1983. This paper is declared a work of the U.S. Government and therefore is in the public domain.

*Structures Research Engineer.
†Senior Principal Engineer.
‡Aerospace Engineer.

Fabrication of René 41

Honeycomb Sandwich

An important mass-saving characteristic of the integral-tank/hot-fuselage design of Ref. 4 is the very low density honeycomb core (1.0% solidity) which stabilizes the high-strength René 41 face sheets. Initial surveys revealed that braze alloys commonly used with René 41 either severely eroded the very thin core material (0.0015 in.) or degraded the physical properties of the René 41. Fourteen braze alloys and their associated temperature cycles were evaluated to identify an alloy which would 1) minimize erosion of the core, 2) provide acceptable flow and filleting, 3) be low in cost, and 4) have a braze temperature cycle compatible with the solution heat treat and aging cycle used to strengthen René 41 (braze at 1950°F and age 1 h at 1700°F, for example).

One braze alloy which costs $26/lb nearly met the above criteria. The composition of this alloy was varied until low corrosion, good flow, and controllable filleting were demonstrated. The chemistry of this new alloy is 69.8Ni-19.7Mn-5.9 Si-4.5Cu. Although many braze alloys contain boron to increase wetability, boron was found to embrittle the René 41 foil. The photomicrograph (165X) of a core-to-face-sheet joint shown in Fig. 2 illustrates the absence of corrosion and the good filleting achieved when brazed at 1975°F. Because of the low cost and absence of corrosion of the modified alloy, this system was used to fabricate the test items discussed in this paper. This braze alloy is now commercially available as AMI 937.

Preliminary Design

Allowables

Structural design data were needed to allow the low-density René 41 honeycomb sandwich to be used with confidence. The types of specimens shown in Fig. 3 were fabricated and tested, either in an as-fabricated condition to obtain initial strengths, or after exposure to thermal cycles under static load to obtain residual strengths. The figure summarizes the types of tests, the maximum temperature and number of different thermal cycles, the range of constant stress applied to different specimens, and the test temperatures. The tests included face tension, core shear, edgewise compression, barrel compression (a test which combines edgewise compression and flatwise tension), flatwise tension, and peel strength. The figure indicates the general magnitude of the test program; a complete breakdown of specimens and specific exposure and test conditions is given in Ref. 7. The test matrix totals 589 tests, including replicates. While this level of effort obviously falls short of establishing a comprehensive data base for handbook-type allowables, it is adequate to provide data for use in preliminary design. Examples of the type of results obtained are shown in Figs. 4-6.

Core Shear

Figure 4 shows core shear ultimate strength (as fabricated) as a function of test temperature. The data are for two densities, two cell sizes, and two core heights. The "square cell" honeycomb core (which is slightly diamond shaped) is fabricated from 0.0015-in. corrugated foil. The core is welded at the foil attachment nodes, and braze alloy does not flow the full length of the core nodes. The solid curves are faired through the average test data. The predicted curves are based on extensive test data for "square cells" with relatively large fillets and 100% braze alloy flow along the core foil attachment nodes. The data for the higher density core falls about 10% below the predicted curve. This difference is believed to be primarily due to the test specimens not having 100% braze alloy node flow, but may be partially a result of scatter and the limited number of specimens tested. The data for the lower density core fall between the predicted curves for the two core heights. Any reduction in core shear strength

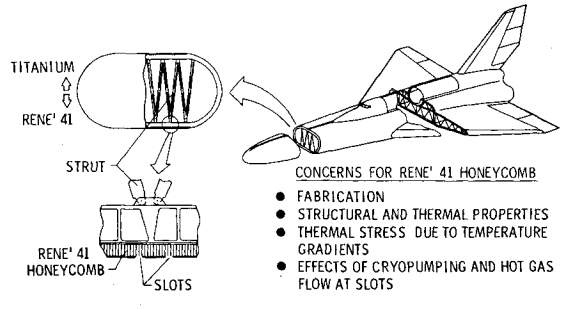

Fig. 1 Integral-tank/hot-fuselage structure concept.

SPECIMEN TYPE →	AS FABRICATED	RESIDUAL STRENGTH									
TEST TYPE ↓	NO. SPECIMENS * TESTED	NO. THERMAL CYCLES UNDER STATIC LOAD **			NO. SPECIMENS TESTED AFTER THERMAL CYCLES						
					TEST TEMPERATURE, °F						
		T_{max}=1400	=1500	=1600°F	-320	75	1000	1200	1400	1500	1600
FACE TENSION	82		100 300 500	100	2	11 3 3	2	9 3 3			5
CORE SHEAR	82	100 200 500	100 200 500			12 12 12			4 4 4	8 8 8	
EDGEWISE COMP.	48	100 200 500	100 200 500	100 200 500		14 14 13			4 4 4	6 6 5	4 4 4
BARREL COMP.	25	100				5	5	5			5
FLATWISE TENSION	33			100		6					6
PEEL STRENGTH	10	500		500		5					

* TEST TEMPERATURES VARY FROM -65°F TO 1600°F
** 1 CYCLE = RT→T_{max}→RT: STATIC LOAD VARIED FROM 10 ksi TO 90 ksi FOR DIFFERENT SPECIMENS

Fig. 3 René 41 honeycomb sandwich allowables tests.

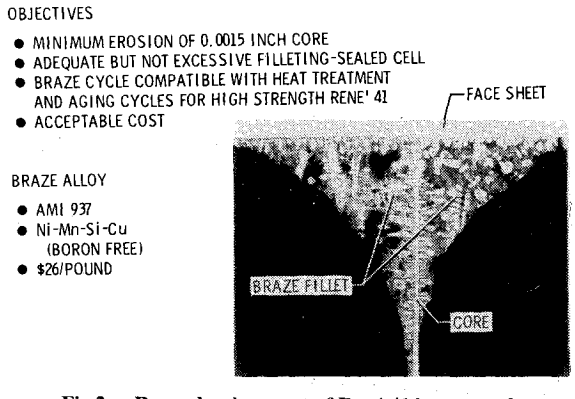

Fig 2. Braze development of René 41 honeycomb.

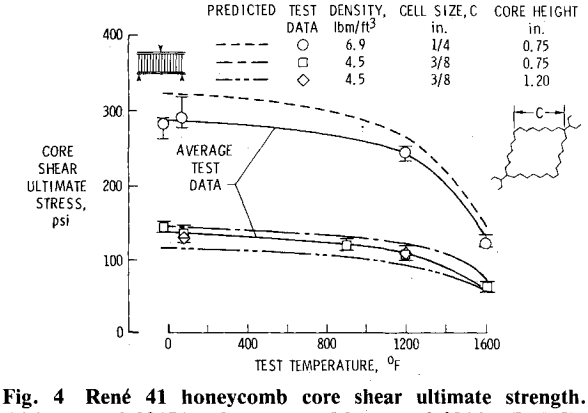

Fig. 4 René 41 honeycomb core shear ultimate strength. Foil thickness = 0.0015 in., face sheet thickness = 0.021 in. (Ref. 7).

associated with an increase in core height (compare square and diamond symbols) cannot be defined because of data scatter.

Thermal Cycle Failure

Figure 5 shows sustained edgewise compressive stress as a function of thermal exposure cycles-to-failure. The data were generated by applying a constant mechanical load to the test specimens and exposing the specimens to the thermal cycle shown in the figure. Initial tests identified several problems. Erosion of the core occurred from interaction (at 1500°F and higher) between the core foil and the potting compound used to stabilize the edges, and undesirable thermal stresses were created near the edges where the load heads contacted and cooled the specimens. After the test specimens and test setup were modified to reduce the effects of these problems, the data shown in Fig. 5 were generated. A face-wrinkling type of failure due to creep occurred in the central portion of the specimens (away from the load heads). As would be expected, the specimens exposed to lower sustained compression stress exhibited greater cycle life. These test results were extrapolated using Larsen-Miller-type creep relationships to identify threshold stresses that could not be exceeded during exposure of the residual-strength test specimens.

Edge Compression

Figure 6 shows edge compression strength as a function of test temperature for the honeycomb geometry identified in the sketch. The data are for as-fabricated specimens and for residual strength specimens which were exposed to 100 thermal cycles with a maximum temperature of 1400°F and with a constant applied stress of 10 ksi prior to testing. The duration of each thermal cycle was about 13.5 min, and included 6 min at 1400°F. The test data is above the compression yield curve, except at 1600°F, and is significantly above the predicted intracell buckling curve. The failure mode was not intracell buckling, but face sheet wrinkling. The prediction for intracell buckling is conservative in that it assumes simply supported edges and neglects the effect of braze alloy and braze alloy fillets. The data points at 1600°F were affected by the corrosive action of the potting compound used to stabilize the ends. Although the corrosion problem was subsequently resolved, this data point was not repeated. The residual strengths shown by the solid symbols in Fig. 6 were consistently equal to the strengths of the as-fabricated specimens. The data points shown are the average of at least three test values. Not all edgewise compression test data showed such consistent results.

Variability of Results

Test specimens were fabricated from core foil supplied by two different vendors. The data in Figs. 4-6 are from specimens fabricated from one vendor. Test data from specimens fabricated from a second vendor exhibited significant scatter, and results often were not consistent. Inspection of the failed specimens showed that core foil from the second vendor had become severely embrittled during exposure to 200 or more thermal cycles peaking at 1500°F as compared to the foil from the first vendor. Photomicrographs showed that surface reactions on each side of the foil from the second vendor extended to a depth of approximately 20% of the foil thickness while surface reactions on foil from the first vendor were almost nonexistent. The exact cause of the surface reaction has not been determined. Foil from the first vendor was furnished with a uniform oxide coating with a definite yellow cast, while foil from the second vendor was furnished in a bright silver satin finish. The bright foil was preoxidized at 1600°F and then brazed to form sandwich test specimens.

Even though some data exhibited large scatter, it can be generally concluded that residual strengths after cyclic

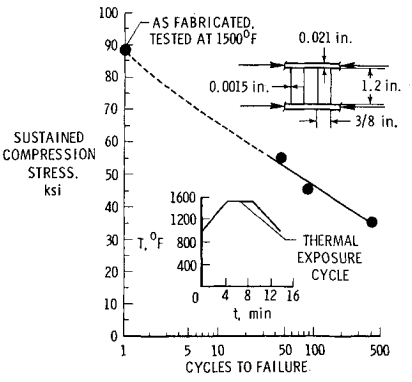

Fig. 5 Edgewise compression life prediction under thermal cycles (Ref. 7).

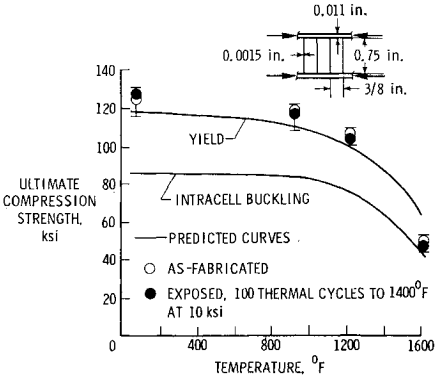

Fig. 6 René 41 honeycomb edgewise compression strength (Ref. 7).

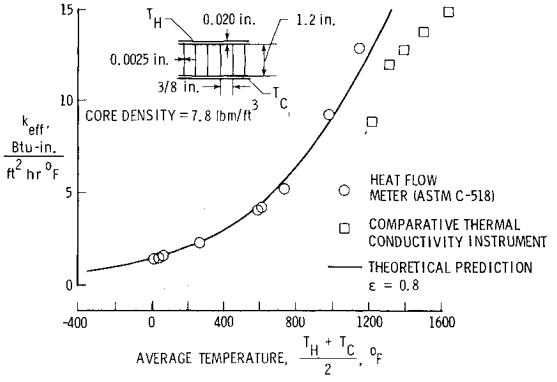

Fig. 7 Effective thermal conductivity of René 41 honeycomb panel (Ref. 10).

thermal exposure decreased with increasing exposure temperature, with increasing stress level, and with increasing number of exposure cycles, but remained at acceptable levels.[7] Data of the type presented in Figs. 4-6, which characterize the more consistent results in Ref. 7, have been used in the studies of Refs. 4 and 8 to establish concept weights. For all of the design allowable results obtained from the test matrix of Fig. 3 see Ref. 7.

Thermal Conductivity

Since the René 41 honeycomb sandwich is exposed to both the low temperatures of cryogenic fuels and the high temperatures associated with entry, the effective thermal conductivity through the thickness of the René 41 honeycomb sandwich was determined over a wide temperature range. The effective thermal conductivity of a medium-density

honeycomb sandwich is shown in Fig. 7 as a function of average temperature. A heat flow meter was used to obtain the circular data points, and a comparative thermal conductivity instrument was used for the higher temperature region to avoid exceeding the power limits of the heat flow meter. Both test systems used guard heaters around the edges of the specimens to minimize heat losses. The heat flow meter data are in excellent agreement with theoretical predictions made using the approach presented in Ref. 9 with an emissivity of 0.8. The test data at the higher temperatures are, on the average, 25% lower than the predicted values. This difference may be due to differences between the two specimens or differences between the two test methods. A comprehensive description of the tests, data, and details of the theoretical predictions are given in Ref. 10. Comparison of the test data shown in Fig. 7 with the theoretically predicted curve indicates that the analytical method provides reasonable definition of the effective thermal conductivity of the René 41 honeycomb sandwich.

Thermal conductivity data were obtained for temperatures in the cryogenic range, but the accuracy of the data is questionable because of a suspected error in wattmeter readings. The data are not shown in Fig. 7, but they are included in Ref. 10 where they are discussed in detail. Additional tests will be required to establish a broader data base and to confirm the effective conductivity at cryogenic temperatures.

Combined Thermal and Mechanical Load Panel Tests

Because thermal stresses are induced by an applied strain rather than an applied force, thermal stresses induced in the plastic range will be less than they would be for the same thermal strain in the elastic range. Furthermore, if the allowable deformation of a structure is large, and the structural stability is not critical, a benign type of failure may occur in which a large part of the thermal stresses is relieved at maximum loading (although significant residual stresses may remain after unloading). Therefore, it has been recommended that for critical conditions involving combined mechanical and thermal loads, the factor of safety used to arrive at ultimate load be applied only to the mechanical load and not to the thermally induced component, regardless of how they are combined.[11] The use of lower load factors for thermal loads can result in higher allowable operating stresses for mechanical loads, which will save mass. In addition, for a limited-life vehicle these operating stresses may even be in the plastic range which can result in even greater mass saving.

Two Rene′ 41 honeycomb panels, each 1×6 ft, were tested under combined thermal and bending loads. The design and fabrication of these panels are documented in Ref. 12. The purpose of the tests was to evaluate the life of a panel when exposed to cyclic combined thermal and mechanical stresses representative of high elastic stresses seen at a fuselage frame attachment and to explore the effect on panel strength of increasing these stresses beyond the proportional limit.

Test Apparatus and Loads

A schematic of the test apparatus and the thermal loads for both boost and entry cycles representative of the trajectories associated with the STS vehicle studied in Ref. 4 are shown in Fig. 8. Quartz lamp heaters were used to produce the desired temperature histories. For safety reasons, the cryogenic temperature (-423°F for LH_2 fuel) required on the inner face sheet during the ascent cycle was represented by using LN_2 at -320°F. The use of LN_2 in place of LH_2 had only a small effect on the thermal strains which occur during the test. Nevertheless, hot surface temperatures were slightly increased to provide equivalent thermal strain levels to account for the small strain difference associated with using the warmer LN_2. The test panel was slightly submerged into the LN_2, and

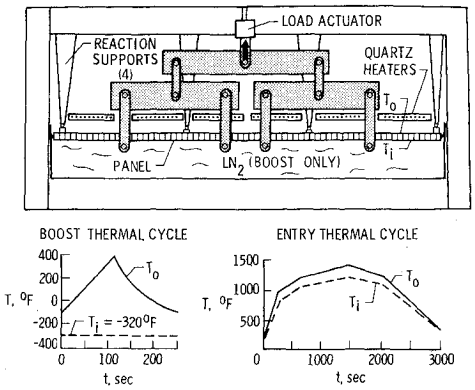

Fig. 8 Combined thermal and mechanical loads—test apparatus and loads.

aluminum tape and fibrous insulation was used around the edges of the panel to prevent the liquid from contacting the core. The panel was instrumented on both face sheets with thermocouples, strain gages, and deflectometers. Strain gages located to measure strain on the hot (compression) side at the reaction supports were usually located 1.0 in. from the centerline of the support to avoid interference with the support.

The maximum outside surface temperature, T_o, for the boost cycle is only 400°F compared to 1400°F for the entry cycle. The temperature difference between the inner and outer skins during boost (720°F) is much larger than the 200°F temperature difference during entry when the cryogenic fuel has been exhausted. As a consequence, the boost cycle is a more critical condition even when changes in material properties due to the high entry temperatures are considered.

Mechanical loads representing fuel pressure loads were applied to the panel through the distribution system shown shaded in the figure. Four line-load supports reacted the applied loads. The two internal reaction supports simulate the reaction forces which would result from fuselage frames reacting thermal and fuel pressure loads in a vehicle. The simulation is incomplete in that at these reaction points the honeycomb core is exposed to compression rather than a net tension load, and the panel is not totally constrained from bowing in the transverse direction as it would be if it were continuously attached to a frame. (However, the loads which react the mechanically applied loads do tend to flatten the panel in the transverse direction.)

Test Results for Panel 1

Selected results from the tests of panel 1 (and panel 2) are given in Table 1. The table identifies the number of accumulated thermal cycles, applied mechanical load, and the maximum longitudinal strain in the skin for selected tests. The panel was exposed to mechanical load and thermal load separately prior to exposure to combined loads.

After the separate load tests, the first panel tested was exposed to 500 boost cycles and 500 entry cycles by alternating between the type of tests in groups of 1, 49, 50, 100, 100, and 200. For each cycle, the mechanical load was held constant while the thermal load indicated in Fig. 8 was applied. During the test program, lamps were adjusted and curtains added to achieve a more uniform temperature distribution on the hot surface, and the emission of the panel surface changed. The resulting changes in surface temperature distribution caused the maximum strains to vary slightly. The maximum compressive strains were between 60 and 80% of the proportional limit. After the first entry cycle, a small bow in the panel in the longitudinal direction was observed. This residual bowing gradually increased with additional exposure to entry cycles, but it was unaffected by additional boost cycles. No damage occurred as a result of the 500 boost and entry cycles, but the

Table 1 Selected René 41 honeycomb panel test results

Panel	Load condition	Accumulated thermal cycles: Boost	Accumulated thermal cycles: Entry	Mechancical load per point, lbf	Maximum skin strain at interior support, microstrain: Outer[a] Measured	Outer[a] Calculated	Inner Measured	Inner Calculated
1	Mechanical only	0	0	980	−350	−450	526	650
	Thermal only	1	0	0	−1770	−2180	2549	2720
	Combined mechanical and thermal load	2	0	980	−2380	−2630	2920	3370
		500	300	980	−1800[b]	−1850[b]	2500	2900
		531	500	2060	−	−2350[b]	2720	3620
		532[c]	500	3300	−2080[b]	−2920[b]	3510	4440
2	Mechanical only	0	0	908	−400	−535	430	635
		0	0	1575	−620	−860	744	1020
	Thermal only	1	0	0	−2220	−2020	2275	2200
	Combined mechanical and thermal load	2	0	980	−2770	−2555	2762	2835
		81	0	1575	−2810	−2880	2981	3220
		152	0	2025	−3000	−3125	3181	3510
		177	0	2475	−3400[d]	−	3357	−
		202	0	2700	−3480[d]	−	3370	−
		252	0	3267	−4000[d]	−	3624	−
		253[e]	0	5000	−8150[f]	−	4761[d]	−
	Entry tests							
1	Mechanical only	0	0	206	−55	−95	88	137
	Thermal only	2	1	0	−	−1470	1210	1650
	Combined mechanical and thermal load	2	2	206	−	−1565	1316	1787
		500	500	206	−	−1565	1470	1787

[a] Maximum compression strain at 1 in. from support centerline.
[b] Maximum compression strain at 1.7 in. from support centerline.
[c] Premature failure, core crushing.
[d] Greater than proportional limit strain.
[e] Large permanent deformation at interior supports.
[f] Greater than yield strain of 5670 microstrain at 400°F.

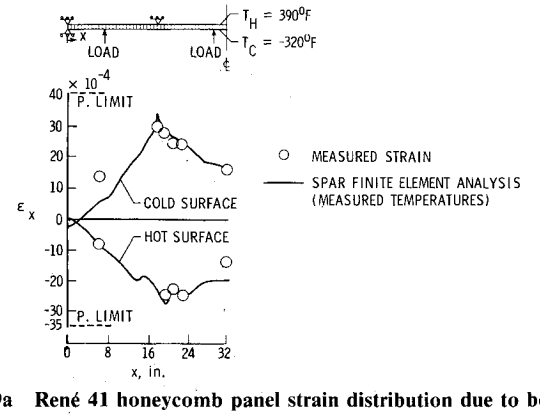

Fig. 9a René 41 honeycomb panel strain distribution due to boost-to-orbit thermal/mechanical loads, panel 1.

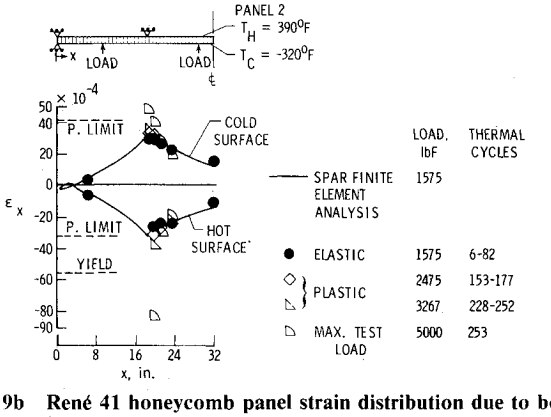

Fig. 9b René 41 honeycomb panel strain distribution due to boost-to-orbit thermal/mechanical loads, panel 2.

panel was left with a permanent center displacement of 0.58 in. over the length of 6 ft with the concave face on the hot side. A force of 210 lbf was required at each load point to elastically straighten the panel. The resulting residual tension stresses on the hot side were 10,400 psi at the support and 16,000 psi at the center of the panel. The cause of the bowing is not understood. A possible cause is a slight shrinkage of the hot face sheet which may occur during the 1400°F entry cycle exposure as a result of additional aging of the René 41 material, but this has not been confirmed. (The panel was originally aged for 1 h at 1700°F and furnace cooled after a 1975°F braze cycle.)

Additional boost cycles (beyond 500) were imposed on the panel with increasing mechanical load until a failure was achieved during cycle 532. The panel failed prematurely by core crushing directly beneath an interior reaction support. This was a nonrepresentative failure mode because, as previously mentioned, the test fixture placed the core in compression while the load pattern at a vehicle fuselage frame would place the core in tension. In addition, the failure is nonrepresentative because the reaction loads were concentrated over a small area to minimize the shading effect from the quartz lamps during heating cycles. The test fixture was modified by increasing the contact area of the reaction loads prior to testing the second panel.

Test Results for Panel 2

Initial separate mechanical and thermal load tests for the second panel were similar to those for the boost tests for the first panel. Because the boost cycle is the more critical cycle, the second panel was subjected only to boost tests. The mechanical load was periodically increased as the number of accumulated boost cycles increased. The measured strain level exceeded the proportional limit for all cycles after cycle 152,

and reached a value about 1.5 times greater than the proportional limit by cycle 252. The panel survived these cycles with no effect, except for plastic deformation which occurred in the region of the reaction supports. The panel was loaded on cycle 253 by increasing the mechanical line loads to the limit of the actuator (5000 lbf). Although the panel showed evidence of permanent set caused by large plastic compression strain of the hot side face sheet in the region of the reaction supports, it continued to carry the load. The maximum compressive strain, measured 1 in. from the support centerline, was about 1.5 times greater than the yield strain. Extrapolation to the centerline would result in an even larger strain.

Comparison with Analysis

Representative strain data for panels 1 and 2 are shown in Fig. 9 and are compared with a strain distribution calculated using the SPAR finite element structural analysis computer program.[13] Measured temperatures were used for the linear analysis. Figure 9a shows results for panel 1 for the second boost cycle, and Fig. 9b shows results for panel 2 for several different cycles, each with higher strain levels. The measured and calculated strains in the elastic range resulting from the combined thermal and mechanical loads are in good agreement. The strains on the hot and cold surfaces are different because the thickness of the hot face sheet for panel 1 was chem-milled to provide an increased thickness in the regions of the reactions. Additionally, the temperature distributions on the two surfaces were different. Temperatures on the LN_2 side were relatively constant since they were influenced by boiling against the specimen surface. The upper surface was hotter in the middle of the specimen than at the edges and at the supports. The maximum strains in the elastic range are about 80% of the proportional limit for panel 1 and 92% of the proportional limit for panel 2. The non-circular data points in Fig. 9b show maximum strains into plastic range for the last 101 boost cycles, which include a level 1.5 times greater than the proportional limit for the last 24 cycles.

These test results indicate that structural behavior of the honeycomb sandwich under high combined thermal and mechanical bending loads may be forgiving. Such a forgiving behavior would allow the panels to be treated as a ductile system in the design process and to be designed to operate at stresses higher than those which would limit design under purely mechanical loads.

Evaluation of Slots in Boost and Entry Thermal Environment

Two additional René 41 honeycomb test panels were fabricated, each with several slots in the outer skin. The purpose of the tests of the first panel was to evaluate the effects of the slots in the boost environment, and the purpose of the tests of the second panel was to evaluate the effect of the slots in the entry environment.

Boost Environment

The first panel was $21 \times 25 \times 1.2$ in. in size. A frame was brazed to the inner skin on the panel centerline. The frame held the sandwich panel flat in the region of the centerline. Thus, the thermal stresses which occur in this region are representative of the thermal stresses that would exist in the integral fuselage structure of the vehicle studied in Ref. 4. About half the slots in the outer skin were open and half were covered with a 0.5-in.-wide strip of 0.010-in.-thick René 41 electron beam welded to the skin along one side of the slot. The cover displays a technique which may be required to reduce high local heating to the sandwich during entry. The panel formed the bottom of a container which was partially filled with LH_2. The panel was supported in the container at the center frame and at each end of the panel. A 0.015-in. Hastalloy X seal was welded to the panel edge and to a frame at the bottom of the container. A schematic of the test fixture (Fig. 10) shows the container covered with foam insulation to minimize boiloff of LH_2. Quartz lamps were used to expose the panel to the boost heat cycle shown in Fig. 10.

The panel was subjected to 36 boost thermal cycles. Figure 11 summarizes the temperature history of the inner and outer surfaces during the 36 cycles. Hold times between cycles ranged from 10 min to 1 h during which cryodeposits accumulated on the panel surface and in the slots. Motion pictures were taken at 16 frames/s during the first cycle and at 1 frame every 6 s during all cycles. The surface temperature during the first cycle exceeded the 400°F design temperature by more than 300°F because frost accumulated on a feedback control thermocouple, insulating it from the radiant heaters. Analysis indicates that plastic strain occurred during this severe condition. The panel was inspected after cycle 10 and cycle 30, and no damage to the panel was observed, although some cracking of the foam insulation around the container was noticed. After 36 cycles, a fire occurred in the test fixture but caused no damage to the panel. The cause of the fire was

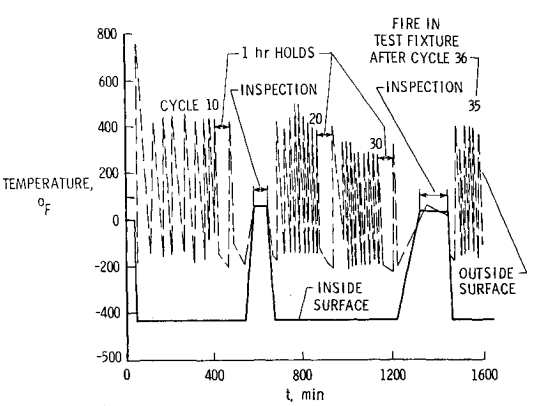

Fig. 11 René 41 honeycomb boost cyclic test temperature history (Ref. 14).

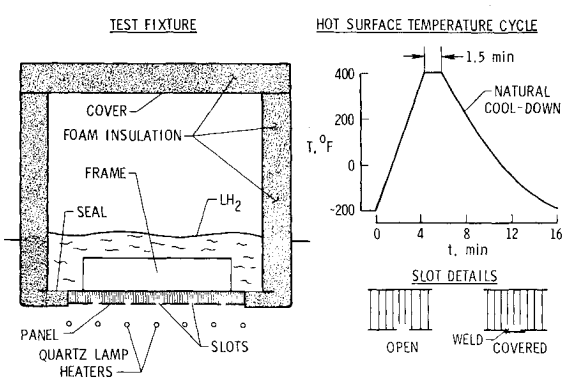

Fig. 10 Cryogenic and boost heating test details.

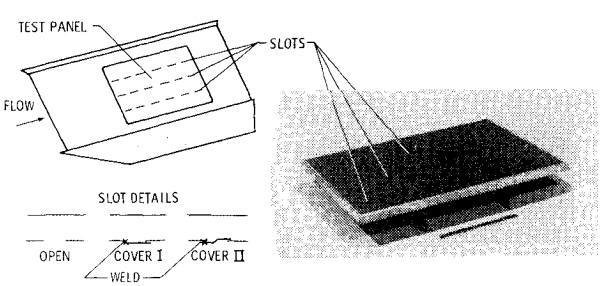

Fig. 12 Mach 7 aerothermal test model.

attributed to an undefined ignition source which could have ignited either gaseous hydrogen, which was leaking out at the lid-container interface, or the foam insulation in the presence of the liquid oxygen component of liquid air condensed in the cracks in the insulation. (The lid-container interface was not tightly sealed for fear that if the vent stack could not accommodate all LH_2 boiloff, a pressure greater than 1 psi might occur and damage the panel seal.) Completion of 36 cycles achieved all test goals except the demonstration of 100 cycles. The costs to repair the test fixture and continue testing compared with an assessment of the need for the remaining 64 cycles led to a decision to stop testing. The panel was examined visually and by x ray and c scan. Sections cut from the panel were examined by metallographic inspection. No structural damage was found.

During the hold times water frost was observed depositing on the $-200°F$ panel surface, and temperatures less than $-300°F$ measured during the tests indicated that liquid air formed in the regions of the core open to the atmosphere. There was no observable or measurable damage to the panel whether the outer skin slots were open or covered. However, the results indicate that additional attention must be given to sealing honeycomb core splices to prevent passage of air into the core from the slots. Without such sealing, considerable liquid oxygen may flow within the honeycomb structure. The results also show that a honeycomb core sandwich with a slotted outer skin integrally fixed to an inner frame can withstand not only the localized thermal environment imposed by the boost trajectory for the Ref. 4 vehicle, but also the more severe environment imposed by the unintentional temperature overshoot of the first cycle. These tests are documented in Ref. 14.

Entry Environment

The purpose of the tests of the second panel is to evaluate the effect of localized heating in the region of the slots during entry. The $22 \times 34 \times 1.2$ in. panel shown in Fig. 12 is designed to be exposed to a Mach 7 stream in the Langley Research Center 8-Ft High Temperature Structures Tunnel (8′ HTST). Two slot cover concepts will be evaluated in addition to the open slot. The panel will be instrumented with thermocouples on the inner face sheet directly beneath the slots and between slots so that the different cover concepts can be compared.

Recommendations for Future Work

The Introduction to this paper describes a future STS concept which uses an integral tank/fuselage hot structure and identifies several concerns which have been addressed in this paper. However, other concerns remain to be addressed. Hydrogen embrittlement of René 41 may be of concern, particularly in welded joints. Joining methods, particularly welding, for René 41 and for dissimilar metal joints, need to be developed. Welded René 41 honeycomb panels require tests to determine strength and life, and to verify leak-free joints. More analytical and experimental work is needed on thermal stresses in builtup structures if advantage is to be taken of the forgivable nature of thermal strains.

Concluding Remarks

Based on the work presented in previous system studies and the hardware development described herein, René 41 honeycomb sandwich appears to be a viable structural concept for an integral cryogenic tank/fuselage hot struture. A fabrication process for René 41 honeycomb with a core density less than 1% has been developed which is consistent with desirable heat treatment processes for high strength. Such a lightweight core enhances the feasibility of the integral-tank/hot-fuselage structural concept having an acceptable mass fraction for future STS. Preliminary structural allowables and thermal properties suitable for system design studies have been determined. Results of tests with combined thermal and mechanical stresses indicate that due to the forgiving nature of thermal stresses, the panels may be treated as a ductile system in the design process and may be designed to operate at stresses higher than those which would limit design under purely mechanical loads. The effects of slots in the outer face sheet on the lower surface of the vehicle have been evaluated in the cryogenic environment associated with containing LH_2 fuel. Cryodeposits which accumulated in the slots during the "ground-hold" period of the tests caused no identifiable damage, even when the exterior surface was subjected to the boost heating trajectory. Wind tunnel tests are planned to evaluate potential high local heating at the slots during entry. A cycle life of 500 missions appears to be a reasonable goal, but additional work is required to complete the assessment of the structural viability of the concept. This work includes hydrogen embrittlement of René 41, evaluation of development of joining methods, and the study of thermal stresses in builtup structures.

References

[1]Kelly, H. N., Rummler, D. R., and Jackson, L. R., "Research in Structures and Materials for Future Space Transportation Systems —An Overview," *Journal of Spacecraft and Rockets,* Vol. 20, Jan.-Feb. 1983, pp. 89-96.

[2]Henry, B. Z. and Eldred, C. H., "Advanced Technology and Future Earth-to-Orbit Transportation System," *Space Manufacturing Facilities II (Space Colonies)*, edited by J. Grey, AIAA, New York, 1977.

[3]Haefeli, R. C., Littler, E. G., Hurley, J. B., and Winter, M. G., "Technology Requirements for Advanced Earth-Orbital Transportation Systems," NASA CR 2867, Oct. 1977.

[4]Hepler, A. K. and Bangsund, E. L., "Technology Requirements for Advanced Earth Orbiter Transportation Systems," NASA CR 2878, July 1978.

[5]Taylor, A. H. and Jackson, L. R., "Thermostructural Analysis of Three Structural Concepts for Reusable Space Vehicles," AIAA Paper 79-0874, May 1979.

[6]Stone, J. E. and Koch, L. C., "Hypersonic Airframe Structures Technology Needs and Flight Test Requirements," NASA CR 3130, July 1979.

[7]Hepler, A. K., Arnquist, J., Koetje, E. J., Esposito, J. J., Lindsay, V. E. J., and Swegle, A. R., "Design Data for Brazed René 41 Honeycomb Sandwich," NASA CR 3382, Jan. 1981.

[8]Hepler, A.K. and Swegle, A. R., "Hot-Structure Development Advanced Space Transportation System Application," AIAA Paper 79-0876, 1979.

[9]Swan, R. J. and Pittman, C. M., "Analysis of Effective Thermal Conductivities of Honeycomb-Core and Corrugated-Core Sandwich Panels," NASA TND-714, April 1961.

[10]Deriugin, V., "Thermal Conductivity of René 41 Honeycomb Panels," NASA CR 159367, Dec. 1980.

[11]Deriugin, V., Brogren, E. W., Jaeck, C. L., Brown, A. L., and Clingan, B. E., "Thermal-Structural Combined Loads Design Criteria Study," NASA CR-2102, Oct. 1972.

[12]Hepler, A. K., and Swegle, A. R., "Design and Fabrication of Brazed René 41 Honeycomb Sandwich Structural Panels for Advanced Space Transportation Systems," NASA CR-165801, Dec. 1981.

[13]*SPAR Structural Analysis System Reference Manual,* Vol. 1, NASA CR 158970-1, Dec. 1978.

[14]Hepler, A. K. and Swegle, A. R., "Cryogenic Performance of Slotted Brazed René 41 Honeycomb Panels," NASA CR-3525, 1982.